DOI: 10.1002/ejic.201000918

Influence of the Introduction of Cyanido and Phosphane Ligands in Multifunctionalized (Mercaptomethyl)silane [FeFe] Hydrogenase Model Systems

Ulf-Peter Apfel,[a] Yvonne Halpin,[b] Helmar Görls,[a] Johannes G. Vos,*[b] and Wolfgang Weigand*[a]

Dedicated to Professor Grzegorz Mloston on the occasion of his 60th birthday

Keywords: Silicon / Cyanides / Phosphanes / Iron / Sulfur / Hydrogenase

Cyanido- and phosphane-substituted [FeFe] hydrogenase models are known to show increased basicity of the [2Fe2S] cluster. Following our continued interest in [2Fe2S(Si)] compounds, substitution reactions of such complexes with tetraethylammonium cyanide as well as triphenylphosphane were investigated to yield the respective monosubstituted triphenylphosphane complexes **2a**–**c** and cyanido complexes **3a**–**c**. Cyclic voltammetry was used to investigate the electrocatalytic H_2 formation with acetic acid.

Introduction

Since the structure of the active site of the [FeFe] hydrogenase was determined,[1,2] much attention has been paid to the synthesis of structural and functional model complexes that contain different S–to–S linkers.[3–7] Recently, [2Fe2S(Si)] complexes that contain functionalized (mercaptomethyl)silanes were reported, and the influence of the silicon moiety on the catalytic cycle during electrocatalysis as well as their unique structural features were investigated.[8] Thereby a sulfur···proton interaction was observed, which can be explained by an increased nucleophilicity of the coordinated sulfur atoms,[8] which was also observed for $[Fe_2(CO)_6\{(SCH_2)_2Sn(CH_3)_2\}]$.[9]

It has been reported that replacement of a carbonyl ligand by either cyanide[10] or phosphane[11] leads to increased basicity of the iron atoms in the [2Fe2S] subsite. This enables formation of terminal or bridging hydrides.[12] However, since CN^- ligands in model systems are not protected by the peptide environment,[1] isocyanic acid complexes can be formed, which has been reported in detail for several L_nM–CNH complexes (Scheme 1).[13,14]

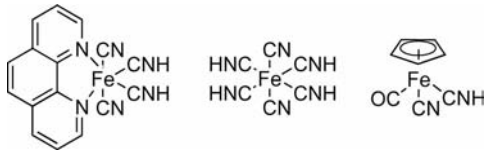

Scheme 1. Isocyanic acid complexes.

In contrast to CN^-, triphenylphosphane is an abiological ligand and cannot be protonated in its coordinated form. Nevertheless, trimethylphosphane reveals a similar donor character and can serve as an abiological surrogate for CN^-.[15]

Inspired by the properties of [2Fe2S(Si)] complexes and the natural abundance of the strong donor ligand CN^-,[16] [FeFe] hydrogenase model complexes **1a**–**c** (Scheme 2) were treated with triphenylphosphane and tetraethylammonium cyanide to afford monosubstituted, asymmetric [2Fe2S(Si)] cluster compounds. The resulting products were investigated according to their chemical and structural properties by cyclic voltammetry and crystal structure analysis.

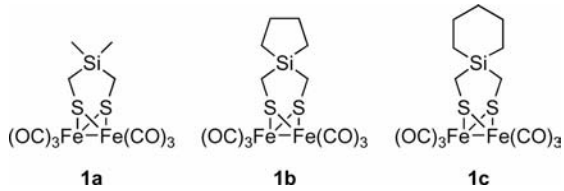

Scheme 2. [2Fe2S(Si)] model complexes **1a**–**c**.[8]

[a] Institut für Anorganische und Analytische Chemie, Friedrich-Schiller Universität Jena,
August-Bebel-Strasse 2, 07743 Jena, Germany
Fax: +49-3641-948102
E-mail: wolfgang.weigand@uni-jena.de
[b] Solar Energy Conversion SRC, School of Chemical Sciences, Dublin City University, Dublin 9, Ireland
E-mail: han.vos@dcu.ie

Results and Discussion

Synthesis and Characterization of PPh_3-Substituted Diiron Complexes 2a–c

Initial experiments to obtain the PPh_3-substituted complexes **2a**–**c** by means of treatment of the hexacarbonyl complexes **1a**–**c** with triphenylphosphane at room temperature[17] or in toluene heated to reflux[18] required long reaction times and showed only partial conversions. A fast and selective exchange of CO was established by oxidative abstraction of CO by using trimethylamine *N*-oxide, followed by addition of triphenylphosphane (Scheme 3).[19]

Initial reaction of trimethylamine *N*-oxide with complexes **1a**–**c** in acetonitrile yields the respective acetonitrile complexes through decarboxylation.[20] Attempts to isolate the unstable nitrile complexes failed, and the synthesis was therefore performed as a one-pot reaction. Further treatment of the in situ formed acetonitrile complexes with triphenylphosphane resulted in monosubstituted compounds **2a**–**c**. The identities of **2a**–**c** were verified by elemental analysis, NMR spectroscopy, MS, and IR studies. Thus, mass spectrometry afforded the $[M]^+$ peaks at m/z = 664 (**2a**), 690 (**2b**), and 704 (**2c**). IR spectroscopy provided additional confirmation for the structures of **2a**–**c**: ν_{CO} bands are visible between 2041 and 1930 cm^{-1}. Single-crystal X-ray analysis revealed the proposed structures as depicted in Figure 1. The iron atoms in **2a**–**c** are coordinated in a distorted octahedral fashion by the S–to–S linker and by CO groups and triphenylphosphane in the equatorial position. The Fe2–P1 distances and the bonding angles (Fe1–Fe2–P1) of **2a**–**c** are the same within the standard deviation and are in good agreement with the recent reported complex $[Fe_2(CO)_5(PPh_3)\{(SCH_2)_2CHOH\}]$.[21] Short Fe–Fe bonds are detected within all three molecules and reveal bond lengths of 250.81(6) (**2a**), 251.16(5) (**2b**), and 249.68(5) pm (**2c**) (cf. Table 1). The silicon atoms exhibit a tetrahedral geometry. However, the angles S1–C1–Si1 and S2–C2–Si1 are about 120° and therefore much larger than the expected 109.5° for sp^3 hybridization (cf. Table 1).

Table 1. Bond lengths [pm] and angles [°] for compounds **2a**–**c**.

	2a	**2b**	**2c**
Fe1–Fe2	250.81(6)	251.16(5)	249.68(5)
Fe2–P1	224.30(9)	225.60(8)	223.71(7)
Fe1–S1	226.69(9)	227.71(7)	226.91(7)
Fe2–S2	229.26(9)	226.21(8)	227.44(7)
S1–C1	183.0(3)	182.1(3)	181.21(3)
S2–C2	182.3(3)	182.9(3)	183.5(3)
C1–Si1	188.1(4)	187.5(3)	186.0(3)
C2–Si1	186.6(4)	186.3(3)	186.1(3)
Si1–C3	186.3(4)	188.5(3)	186.1(3)
Si1–C4/C6/C7	186.2(4)	188.6(3)	186.7(3)
S1–Fe1–S2	86.18(3)	85.80(3)	86.66(2)
S1–Fe2–S2	86.30(3)	86.08(3)	86.45(2)
Fe1–Fe2–P1	156.74(3)	156.66(3)	156.26(3)
S1–C1–Si1	122.05(19)	120.08(15)	121.76(15)
S2–C2–Si1	118.37(18)	117.65(15)	119.30(13)
C1–Si1–C2	108.19(15)	108.29(13)	108.09(12)
C1–Si1–C3	112.85(18)	115.41(14)	113.82(13)
C3–Si1–C4/C6/C7	108.58(18)	95.22(15)	103.63(13)

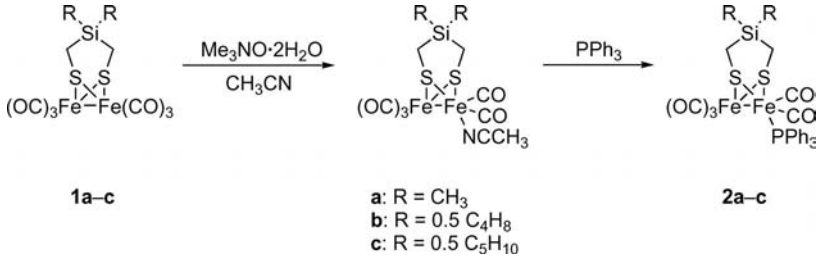

Scheme 3. Reaction pathway towards monosubstituted compounds **2a**–**c** containing the PPh_3 ligand.

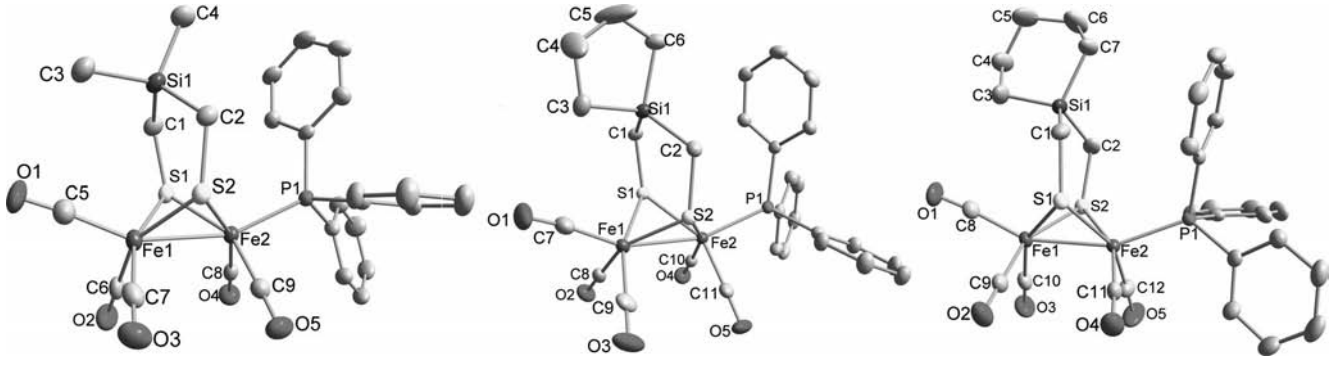

Figure 1. Molecular structures of compounds **2a**–**c** (left to right; ellipsoids at the 50% level). The molecular structure of **2c** shows one of two independent molecules.

Synthesis and Characterization of the CN^--Substituted Diiron Complexes 3a–c

The replacement of a CO ligand by CN^- follows similar procedures[22] as described for the tiphenylphosphane complexes **2a**–**c** and leads to the negatively charged complexes **3a**–**c**. Again, the labile acetonitrile complex is formed first and is easily substituted by the addition of tetraethylammonium cyanide. Further purification affords compounds **3a**–**c** (Scheme 4) as dark red substances.

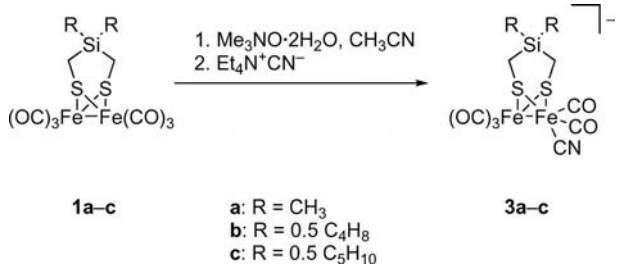

Scheme 4. Synthesis of monosubstituted complexes **3a**–**c** containing the CN^- ligand.

The identities of **3a**–**c** were established by NMR spectroscopy, MS, and IR studies. Consequently, mass spectrometry reveals the $[M]^-$ peaks at *m*/*z* = 428 (**3a**), 454 (**3b**), and 468 (**3c**). IR spectroscopy shows the ν_{CO} bands between 2030 and 1930 cm^{-1} and the ν_{CN} band at around 2088 cm^{-1}. Slow diffusion of hexane into a solution of **3b**, dissolved in thf, at 0 °C affords single crystals suitable for structure determination (Figure 2).

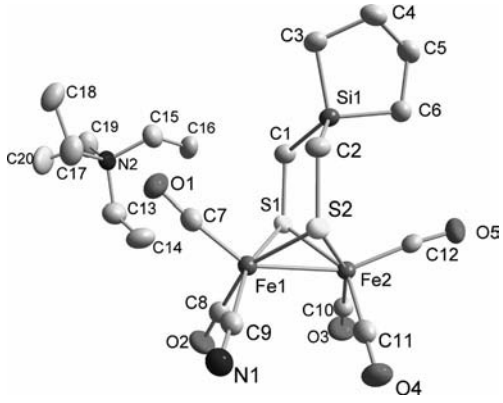

Figure 2. Molecular structure of compound **3b** (ellipsoids at the 50% level). Hydrogen atoms are omitted for clarity.

The molecular structure of **3b** shows the complex anion $[2Fe2S(Si)(CN)]^-$, in which the counterion is a tetraethylammonium cation. The iron atom Fe1 is coordinated by a cyanido ligand in a basal position, two CO ligands, the Fe2 atom, and the dithiolato bridge. Both iron atoms are coordinated in a distorted octahedral way. In contrast to the phosphane complex **2b**, the iron–iron distance is significantly longer (cf. Table 2). The silicon atom is tetrahedrally coordinated, and unusually large bond angles S1–C1–Si1 and S2–C2–Si1 of 118.4(2) and 119.8(2)°, respectively, are observed (see Table 2). The bond lengths for Fe1–C9 and C9–N1 are in good agreement with those reported for $(Et_4N)[Fe_2(S_2C_3H_6)(CN)(CO)_5]$.[3]

Table 2. Bond lengths [pm] and angles [°] for compound **3b**.

Fe1–Fe2	252.32(8)	C2–Si1	186.9(4)
Fe1–S1	224.82(11)	Si1–C3	187.5(4)
Fe2–S2	227.36(10)	Si1–C6	187.5(84)
S1–C1	182.8(4)	Fe1–C9	193.5(4)
S2–C2	183.0(4)	C9–N1	115.4(5)
C1–Si1	187.3(4)		
S1–Fe1–S2	88.49(4)	C1–Si1–C2	106.57(18)
S1–Fe2–S2	87.22(4)	C1–Si1–C3	112.32(19)
S2–C2–Si1	119.8(2)	C3–Si1–C6	95.64(19)
S1–C1–Si1	118.4(2)	Fe2–Fe1–C9	107.50(13)

Experiments that used two or more equivalents of CN^- or PPh_3 afforded only monosubstituted complexes. An increased electron density at the coordinated CO ligand can be observed due to the σ-donor ability of CN^- or PPh_3 ligands.[23] Further reactions of **1a**–**c** with 1,10-phenanthroline were carried out. By using the same reaction conditions as for **2a**–**3c**, the desired [2Fe2S(phenanthroline)] complex was not obtained;[24] in contrast, decomposition to $[Fe(phenanthroline)_3]^{2+}$ was observed.

IR Spectroscopy

As pointed out, the basicity of the iron centers can be increased by using the strong-field ligands CN^- and PPh_3, whereby CN^- is more relevant in the hydrogenase system.[1,2] The basicity (electron density) of the iron atoms depends mainly on two different aspects: (i) the oxidation state,[18,25] and (ii) the σ/π-bonding properties of the ligands.[10,11] A characteristic feature that can be used to determine the basicity of the iron centers is the ν_{CO}. The smaller the ν_{CO} value, the larger the basicity of the iron centers.[26] The infrared spectroscopic data for complexes **1a**, **2a**, and **3a** are listed in Table 3 and are representative for **1b**–**c**, **2b**–**c**, as well as **3b**–**c**. By evaluating the IR data, a decrease of ν_{CO} can be observed from **1a** to **2a** and **3a**, which show an increased electron density at the iron atoms. Thus, CN^- is the strongest donor ligand in this series. Similar electronic effects have been previously reported for cyanide and phosphane derivatives of $[Fe_2(CO)_4(L)_2(SR)_2]$-type complexes.[3,27]

Table 3. ν_{CO} infrared bands of complexes **1a**–**3a** (KBr pellets).

Compound	ν_{CO}	ν_{CN}
1a[8]	2074 (vs), 2031 (vs), 1989 (vs)	–
2a	2041 (vs), 1981 (vs, b)	–
3a	2027 (vs), 1973 (vs)	2088

Electrochemistry

Cyclic and differential pulse voltammetry were carried out to investigate the electrocatalytic properties of the triphenylphosphane complexes **2a**–**c** and cyanide complex **3c** towards H_2 development. The reduction and oxidation po-

tentials of the complexes are listed in Table 4. We were not able to investigate the electrochemical properties of compound **3a** and **3b**, because of their low solubility in any solvent.

Table 4. Electrochemical data of the hexa- and pentacarbonyldiiron hydrogenase model compounds **1a**–**c**, **2a**–**c**, and **3c**. All potentials are corrected for the $Ag/AgNO_3$ (0.1 M nBu_4NPF_6, 0.01 M $AgNO_3$ in acetonitrile) reference electrode with internal Fc/Fc^+ reference.

Compound	$Fe^IFe^I/Fe^{II}Fe^{II}$ [V]	Fe^IFe^I/Fe^0Fe^0 [V]
1a (acetonitrile)[8]	+0.79 (E_{pa})	–1.40 (E_{pa}) –1.48 (E_{pc})
1b (acetonitrile)[8]	+0.81 (E_{pa})	–1.40 (E_{pa}) –1.48 (E_{pc})
1c (acetonitrile)[8]	+0.81 (E_{pa})	–1.39 (E_{pa}) –1.49 (E_{pc})
2a (dichloromethane)	+0.57 (E_{pa}) +0.44 (E_{pc})	–1.83 (E_{pc})
2b (dichloromethane)	+0.62 (E_{pa}) +0.49 (E_{pc})	–1.80 (E_{pc})
2c (dichloromethane)	+0.61 (E_{pa}) +0.46 (E_{pc})	–1.85 (E_{pc})
3c (acetonitrile)	+0.86 (E_{pa})	–2.04 (E_{pc})

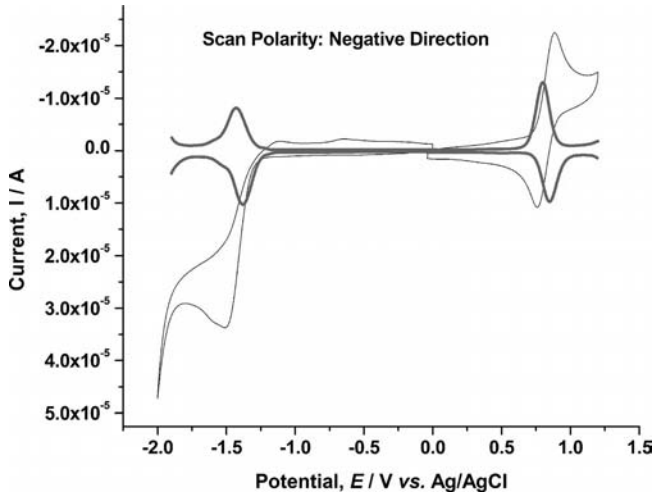

Figure 3. Cyclic voltammetry (black) and differential pulse voltammetry (gray) of compound **2a** (representative also for **2b** and **2c**) [1 mM] on a glassy carbon working electrode, in dichloromethane, by using 0.05 M nBu_4NPF_6 as the supporting electrolyte and Ag/AgCl as the reference electrode.

Triphenylphosphane ligands in **2a**–**c** led to an increased electron density around the diiron center. This is clearly shown by the oxidation and reduction potentials of the three hydrogenase models (cf. Table 4). When comparing the redox potentials of these complexes with their hexacarbonyl analogues **1a**–**c**, and allowing for effects of the different solvent (dichloromethane results in positive shifts compared with the corresponding process in acetonitrile), it is evident that the former are both easier to oxidize and harder to reduce. Upon inspection of the cathodic waves in each of the cyclic voltammograms, a second reduction process is observed that occurs at potentials very close to the first (least negative) reduction process, although not at all clear in the differential pulse. This type of two-electron reduction has been observed for a similar monosubstituted complex, $[Fe_2(bdt)(CO)_5\{P(OMe)_3\}]$ (bdt = 1,2-benzenedithiolate),[28] and may be related to the coordination asymmetry of the two Fe centers in the molecules. The two-electron reduction step coincides well with the hexacarbonyl complexes **1a**–**c**, for which the first reduction signal has been assigned to an electron transfer–chemical reaction–electron transfer (ECE) mechanism.[8] From the cyclic voltammogram in Figure 3, it can be seen that the reversibility of the oxidative process is greatly improved with the PPh_3-substituted complexes. This is, because the σ-donor character of this ligand stabilizes the $Fe^{II}Fe^{II}$ redox state, whereas the reduced state is destabilized by this ligand, as indicated by the irreversibility of the cathodic waves in each cyclic voltammogram.[29] The PPh_3-functionalized complexes are oxidized at potentials approximately 200–250 mV less positive than the hexacarbonyl analogues. However, it must be noted that this is not a direct comparison as the electrochemical solvent used for the PPh_3 complexes is dichloromethane (these complexes were insoluble in acetonitrile), whereas acetonitrile was the solvent for the hexacarbonyl derivatives.

Upon addition of 1 mmol of HOAc to the complexes, the separation of this first cathodic wave into two peaks was observed with a minor positive shift in potential as for the first wave. The second, now more prominent peak experienced a shift of approximately 200 mV towards more negative potentials. An increase in the current of this second cathodic wave was observed, and the process shifted to more negative potentials, with these shifts continuing with each increment of acid added thereafter. It is tentatively proposed that any hydrogen evolved occurs from the Fe^0Fe^0 redox state. This type of behavior is observed for all three of the monosubstituted complexes containing PPh_3 (Figure 4).

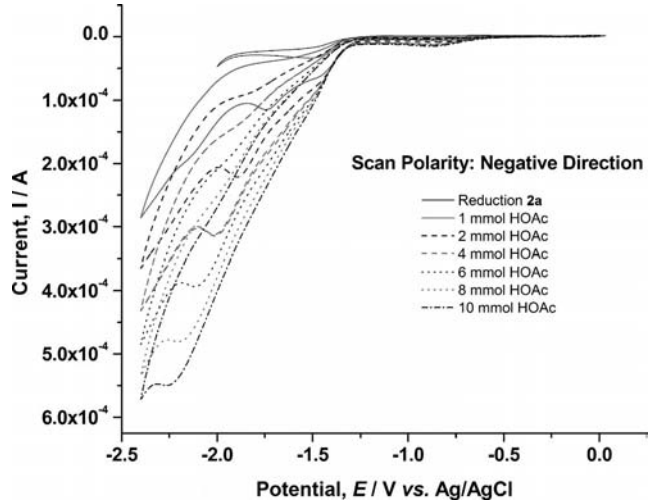

Figure 4. Cyclic voltammetry of **2a** [1 mM] with HOAc (0–10 mmol) in dichloromethane (electrolyte: 0.05 M nBu_4NPF_6), representative also for compound **2b** and **2c**.

The pentacarbonyldiiron complex **3c** was electrochemically investigated by using acetonitrile as solvent. The oxidation wave observed for this complex occurs at a potential

(+0.86 V vs. Ag/Ag^+) that is approximately 50 mV more positive than the corresponding process in the hexacarbonyl analogue **1c** that is oxidized at +0.81 V vs. Ag/Ag^+. This is counterintuitive if one considers the presence of the CN^- ligand, which should increase the electron density around the diiron active site. The complex appears to pacify the electrode with each successive cycle as indicated by the gradual decrease in current.

The increased electron density on the metal atom is reflected in the reduction potential recorded for **3c** (Figure 5). The ($Fe^IFe^I + 2\ e^- \rightarrow Fe^0Fe^0$) is observed at a potential (–2.04 V vs. Ag/Ag^+) that is approximately 500 mV more negative than that of the hexacarbonyl analogue **1c**. A similar negative shift of the reduction potential was already observed for the negatively charged monocyanide $[Fe_2\{\mu\text{-}S_2(CH_2)_3\}(CN)(CO)_5]^-$.[3] However, the reduction potential obtained for compound **3c** is about 300 mV more negative than for the respective propanedithiolato species.

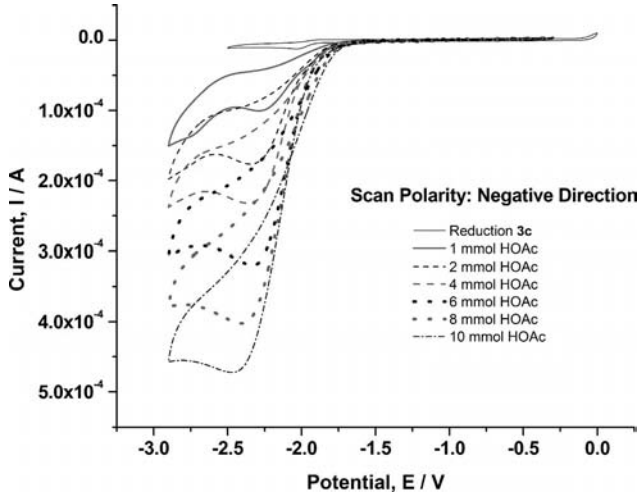

Figure 5. Cyclic voltammetry of compound **3c** [1 mM] with HOAc (0–10 mmol) on a glassy carbon working electrode, in acetonitrile, by using 0.05 M nBu_4NPF_6 as the supporting electrolyte and Ag/Ag^+ as the reference electrode (0.1 M nBu_4NPF_6 and 0.01 M $AgNO_3$ in CH_3CN).

The expected basicity around the iron–iron bond or the nitrile ligand itself in **3c** is not reflected in its electrocatalytic behavior in the presence of acetic acid. The presence of these basic sites led to an increased susceptibility to protonation prior to reduction of the complex, which is indicated by a positive shift in the reduction potential of the least negative cathodic process.[30] Upon addition of 1 mmol of HOAc, the reduction potential of this process shifted by approximately 200 mV in the negative direction, and an increase in the height of the peak was observed. The intensity of the current continued to increase with each increment of acid added thereafter, which is indicative of an electrocatalytic current. These results suggest that the evolution of hydrogen is mediated from the Fe^0Fe^0 redox state. However, the observed catalytic wave is within the region of that observed when acetic acid itself is reduced in the absence of a catalyst (ca. –2.4 V vs. Ag/Ag^+), which was also observed by Darensbourg et al.,[29] and as such it is not possible at this moment to clearly assign this process as hydrogen evolution catalyzed by the FeFe complex. In contrast to the literature-known complex $[Fe_2\{\mu\text{-}S_2(CH_2)_3\}(CN)(CO)_5]^-$, a protonation at the N atom of the cyanide was not observed.[23,31]

Conclusion

Over the course of this study, a suitable synthesis route to monosubstituted asymmetric [2Fe2S(Si)] model complexes that contain triphenylphosphane (**2a**–**c**) and cyanide (**3a**–**c**) was established. Single-crystal X-ray determination revealed a basal configuration mode of the introduced cyanide and an apical for the triphenylphosphane in the solid state. As already shown for **1a**–**c**, the substitution pattern on the silicon atom reveals no or negligible influence on the electrocatalytic cycle.[7] During the investigation of the electrochemical properties, unexpected trends arose in the evaluation of the redox potentials in certain complexes of this series. Addition of σ-donor ligands such as CN^- or PPh_3 led to an increase in electron density around the metal centers, which should result in an increase in basicity of the active site. This theory is not completely consistent with all oxidation potential values obtained. In contrast to results of Poilblanc et al.,[11,32] who showed that complexes $[Fe_2(SR)_2(CO)_4L_2]$ (L = donor ligand) are both easier to oxidize and harder to reduce, monosubstituted cyanido complex **3c** experiences an oxidation potential that is more positive than that of the corresponding hexacarbonyl analogues. Therefore, the effect of these ligands on the nature of the HOMO and LUMO must be considered. The addition of a negatively charged ligand may change the location of these orbitals, thus resulting in a complicated interpretation of results. Both the oxidation and reduction potentials of complexes **2a**–**c** experience shifts in the negative direction. Two closely spaced reduction steps were observed for these compounds. Catalytic behavior was observed for all complexes. However, direct comparison of all six complexes was not possible as a result of solubility issues in different solvents.

Experimental Section

General Procedures: All syntheses were carried out under dry nitrogen or argon. The organic solvents used were dried and purified according to standard procedures and stored under dry argon. Chemicals were used as received from Fluka and Acros without further purification. Compounds **1a**–**c** were prepared according to literature procedures.[8] Thin layer chromatography (TLC): Merck silica gel 60 F_{254} plates; detection under UV light at 254 nm. Flash chromatography (FC): Fluka silica gel 60. ^1H, $^{13}C\{^1H\}$, and $^{31}P\{^1H\}$ NMR spectra were recorded with a Bruker Avance 200 or 400 MHz spectrometer, whereby the multiplicities of proton resonances are defined as s (singlet), d (doublet), t (triplet), and m (multiplet). $CDCl_3$ was used as the solvent. Chemical shifts (δ [ppm]) were determined relative to internal $CHCl_3$ [^1H ($CDCl_3$): δ = 7.24 ppm], $CDCl_3$ [^{13}C ($CDCl_3$): δ = 77.0 ppm], or external TMS [^1H ($CDCl_3$): δ = 0.00 ppm]. Analysis and assignments of the ^1H NMR spectroscopic data were supported by $^1H,^1H$ COSY, $^{13}C,^1H$

heteronuclear multiple quantum coherence (HMQC), and $^{13}C,^{1}H$ heteronuclear multiple bond correlation (HMBC) experiments. Assignment of the ^{13}C NMR spectroscopic data was supported by DEPT 135, $^{13}C,^{1}H$ heteronuclear single quantum coherence (HSQC), and $^{13}C,^{1}H$ HMBC experiments. IR spectra were recorded with a Perkin–Elmer 2000 FTIR spectrometer. Electron impact and atom bombardment mass spectrometry was carried out at 70 eV with a Finnigan SSQ710 by using desorption electron ionization (DEI) or fast atom bombardment (FAB) mode. Elemental analyses (C, H, N, S) were carried out with a Leco CHNS-931 instrument.

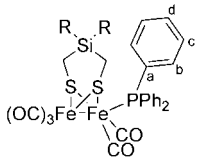

Synthetic Methods

Method A: Replacement of CO by PPh_3 was performed as follows: The hexacarbonyl complex (**1a**–**c**) was dissolved in acetonitrile (20 mL). $Me_3NO{\cdot}2H_2O$ (1 equiv.) was added to give the respective nitrile complex within 30 min, visible by darkening of the red solution. Subsequently, PPh_3 (1 equiv.) was added, and the reaction mixture was stirred at room temperature for 7 h. Concentration to dryness afforded the crude product, which was purified by means of FC (thf/hexane, 1:3).

Method B: A solution of the complex (**1a**–**c**) dissolved in acetonitrile (20 mL) was treated with $Me_3NO{\cdot}2H_2O$ (1 equiv.) and was stirred at room temperature for 30 min. Following that, tetraethylammonium cyanide (1 equiv.) was added, and the solution was stirred for 20 h. Removal of the solvent under reduced pressure afforded the crude product. The residue was dissolved in thf, and the remaining solid was filtered off. Repeated evaporation and washing with hexane afforded the respective cyanide complexes.

Pentacarbonyl(triphenylphosphane)diiron Complex 2a: Compound **1a** (148 mg, 0.344 mmol) was treated with trimethylamine *N*-oxide dihydrate (39 mg, 0.348 mmol) and triphenylphosphane (93 mg, 0.48 mmol) according to Method A to yield **2a** (66 mg, 0.1 mmol, 29%). ^{1}H NMR ($CDCl_3$, 200 MHz): δ = 7.67 (m, 9 H, H-c/d), 7.43 (m, 6 H, H-b), 0.09 (s, 6 H, SiCH_3), –0.31 (s, 4 H, SCH_2Si) ppm. $^{13}C\{^{1}H\}$ NMR ($CDCl_3$, 50 MHz): δ = 213.8/209.4 (CO), 135.8 (C-a), 133.5 (C-b), 130.1 (C-d), 128.5 (C-c), 4.9 (SCH_2Si), 0.5/–0.2 (SiCH_3) ppm. $^{31}P\{^{1}H\}$ NMR ($CDCl_3$, 81 MHz): δ = 68.5 ppm. MS (DEI): *m*/*z* = 664 $[M]^+$, 608 $[M - 2\ CO]^+$, 580 $[M - 3\ CO]^+$, 524 $[M - 5\ CO]^+$, 262 $[PPh_3]^+$. IR (KBr): 3060 (w), 2041 (vs), 1981 (vs, br.), 1628 (m), 1435 (m) cm^{-1}. $C_{27}H_{25}Fe_2O_5PS_2Si$ (663.9): calcd. C 48.81, H 3.79, S 9.65; found C 48.65, H 3.83, S 9.49.

Pentacarbonyl(triphenylphosphane)diiron Complex 2b: Complex **1b** (147 mg, 0.322 mmol) was treated with trimethylamine *N*-oxide dihydrate (36 mg, 0.322 mmol) and triphenylphosphane (84 mg, 0.322 mmol) according to Method A to yield the desired product as a brownish powder (48 mg, 0.07 mmol, 21.6%). ^{1}H NMR ($CDCl_3$, 200 MHz): δ = 7.69 (m, 9 H, H-c/d), 7.41 (m, 6 H, H-b), 1.55–1.24 (m, 8 H, $SiCH_2CH_2C$ and SCH_2Si), 0.65 (t, ^{3}J = 7 Hz, 4 H, SiCH_2C) ppm. $^{13}C\{^{1}H\}$ NMR ($CDCl_3$, 50 MHz): δ = 213.2/209.2 (CO), 136.1 (C-a), 133.4 (C-b), 130.1 (C-d), 128.6 (C-c), 26.9/26.2 ($SiCH_2CH_2C$), 13.8 (SiCH_2C), 3.8 (SCH_2Si) ppm. $^{31}P\{^{1}H\}$ NMR ($CDCl_3$, 81 MHz): δ = 68.7 ppm. MS (DEI): *m*/*z* = 690 $[M]^+$, 634 $[M - 2\ CO]^+$, 606 $[M - 3\ CO]^+$, 550 $[M - 5\ CO]^+$, 262 $[PPh_3]^+$. IR (KBr): 3056 (w), 2925 (s), 2854 (m), 2041 (vs), 1982 (vs, br.), 1630 (m), 1436 (m) cm^{-1}. $C_{29}H_{27}Fe_2O_5PS_2Si$ (689.9): calcd. C 50.45, H 3.94, S 9.29; found C 50.56, H 3.69, S 8.99.

Pentacarbonyl(triphenylphosphane)diiron Complex 2c: Complex **1c** (50 mg, 0.106 mmol) was treated with trimethylamine *N*-oxide dihydrate (12 mg, 0.106 mmol) and triphenylphosphane (28 mg, 0.106 mmol) according to Method A. After purification, **2c** (19 mg, 0.03 mmol, 25%) was obtained. ^{1}H NMR ($CDCl_3$, 200 MHz): δ = 7.63 (m, 9 H, H-c/d), 7.38 (m, 6 H, H-b), 1.53–1.26 (m, 10 H, $CH_2SiCH_2CH_2CH_2$), 0.70 (m, 2 H, SiCH_2) ppm. $^{13}C\{^{1}H\}$ NMR ($CDCl_3$, 50 MHz): δ = 213.8/209.4 (CO), 135.8 (C-a), 133.5 (C-b), 130.1 (C-d), 128.4 (C-c), 29.3 ($SiCH_2CH_2CH_2C$), 23.8 ($SiCH_2CH_2C$), 13.5 (SiCH_2C), 2.9 (SCH_2Si) ppm. $^{31}P\{^{1}H\}$ NMR ($CDCl_3$, 81 MHz): δ = 68.6 ppm. MS (DEI): *m*/*z* = 704 $[M]^+$, 648 $[M - 2\ CO]^+$, 620 $[M - 3\ CO]^+$, 564 $[M - 5\ CO]^+$, 262 $[PPh_3]^+$. IR (KBr): $\tilde{\nu}$ = 3054 (w), 2919 (m), 2852 (m), 2041 (vs), 1981 (vs), 1930 (s), 1637 (m), 1435 (m) cm^{-1}. $C_{30}H_{29}Fe_2O_5PS_2Si$ (703.9): calcd. C 51.15, H 4.15, S 9.10; found C 51.49, H 4.10, S 9.11.

Pentacarbonyl(cyanido)diiron Complex 3a: Compound **1a** (55 mg, 0.128 mmol) was treated with trimethylamine *N*-oxide (14 mg, 0.128 mmol) and tetraethylammonium cyanide (20 mg, 0.128 mmol) according to Method B to yield compound **3a** (41 mg, 0.07 mmol, 57%). ^{1}H NMR (CD_3CN, 200 MHz): δ = 3.19 (m, 8 H, NCH_2C), 1.39 (s, 2 H, SCH_2Si), 1.21 (m, 14 H, SCH_2Si and CH_3), 0.10/–0.05 (2s, 6 H, SiCH_3) ppm. $^{13}C\{^{1}H\}$ NMR (CD_3CN, 50 MHz): δ = 216.9/213.3 (CO), 53.6 (NCH_2C), 8.3 (CH_3), 7.3 (SCH_2Si), –1.0 (SiCH_3) ppm. MS (FAB, neg.): *m*/*z* = 428 $[M - Et_4N]^-$. IR (KBr): $\tilde{\nu}$ = 2924 (m), 2088 (w, CN), 2027 (vs, CO), 1973 (vs, CO), 1630 (m), 1484 (m) cm^{-1}. Elemental analysis data was not obtained.

Pentacarbonyl(cyanido)diiron Complex 3b: Compound **1b** (53 mg, 0.116 mmol) was treated with trimethyalamine *N*-oxide dihydrate (13 mg, 0.116 mmol) and tetraethylammonium cyanide (18 mg, 0.116 mmol) according to Method B to afford **3b** (37 mg, 0.06 mmol, 54%) as a red oily substance. ^{1}H NMR (CD_3CN, 400 MHz): δ = 3.14 (m, 8 H, NCH_2C), 1.45–1.19 (m, 18 H, SCH_2Si, $SiCH_2CH_2C$ and CH_3), 0.65/0.49 (2 m, 4 H, SiCH_2C) ppm. $^{13}C\{^{1}H\}$ NMR (CD_3CN, 50 MHz): δ = 216.8/212.9 (CO), 53.2 (NCH_2C), 27.3 ($SiCH_2CH_2C$), 13.9 (SiCH_2C), 7.8 (CH_3), 6.9 (SCH_2Si) ppm. MS(FAB, neg.): *m*/*z* = 454 $[M - Et_4N]^-$. IR (KBr): $\tilde{\nu}$ = 2982 (s), 2925 (s), 2853 (m), 2087 (w, CN), 2027 (vs, CO), 1974 (vs, CO), 1630 (s), 1484 (m) cm^{-1}. Elemental analysis data was not obtained.

Pentacarbonyl(cyanido)diiron Complex 3c: Compound **1c** (57 mg, 0.12 mmol) was treated with trimethyalamine *N*-oxide dihydrate (13 mg, 0.12 mmol) and tetraethylammonium cyanide (19 mg, 0.12 mmol) according to Method B. Yield: 32 mg (0.05 mmol, 44%). ^{1}H NMR (CD_3CN, 400 MHz): δ = 3.14 (m, 8 H, NCH_2C), 1.57 (m, 4 H, SCH_2Si), 1.19 (m, 16 H, $SiCH_2CH_2C$, $SiCH_2CH_2CH_2C$ and CH_3), 0.88 (m, 2 H, $SiCH_2CH_2C$), 0.74/0.54 (2 m, 4 H, SiCH_2C) ppm. $^{13}C\{^{1}H\}$ NMR (CD_3CN, 50 MHz): δ = 212.4 (CO), 54.1 (NCH_2C), 30.3 ($SiCH_2CH_2CH_2C$), 26.2 ($SiCH_2CH_2C$), 24.6 (SiCH_2C), 8.7 (CH_3), 5.0 (SCH_2Si) ppm. MS (FAB, neg.): *m*/*z* = 468 $[M - Et_4N]^-$. IR (KBr): $\tilde{\nu}$ = 2922 (s), 2089 (w, CN), 2027 (vs, CO), 1973 (vs, CO), 1637 (m) cm^{-1}. Elemental analysis data was not obtained.

Structure Determinations: The intensity data for the compounds were collected with a Nonius KappaCCD diffractometer by using graphite-monochromated Mo-K_α radiation. Data were corrected for Lorentz and polarization effects but not for absorption effects.[33,34] Crystallographic data as well as structure solution and refinement details are summarized in Table 5. The structures were solved by direct methods (SHELXS[34]) and refined by full-matrix

Table 5. Crystal data and refinement details for the X-ray structure determinations of the compounds **2a**, **2b**, **2c**, and **3b**.

Compound	**2a**	**2b**	**2c**	**3b**
Empirical formula	$C_{27}H_{25}Fe_2O_5PS_2Si{\cdot}0.5C_2H_8O_2$	$C_{29}H_{27}Fe_2O_5PS_2Si$	$C_{30}H_{29}Fe_2O_5PS_2Si$	$C_{12}H_{12}Fe_2NO_5S_2Si{\cdot}C_8H_{20}N$
M_r [g mol^{-1}]	696.39	690.39	704.41	584.39
T [°C]	–90(2)	–90(2)	–90(2)	–90(2)
Crystal system	triclinic	triclinic	monoclinic	monoclinic
Space group	$P\bar{1}$	$P\bar{1}$	$P2_1/n$	$P2_1/c$
a [Å]	10.0550(4)	10.4099(5)	16.6325(3)	17.1886(9)
b [Å]	12.8059(4)	12.6449(5)	20.7724(3)	12.5652(6)
c [Å]	13.8444(6)	12.8477(3)	18.3780(5)	12.2768(3)
α [°]	75.360(3)	105.563(2)	90	90
β [°]	77.349(3)	94.001(3)	99.982(1)	100.704(3)
γ [°]	68.226(3)	110.728(2)	90	90
V [Å^3]	1586.08(11)	1498.03(10)	6253.4(2)	2605.4(2)
Z	2	2	8	4
ρ [g cm^{-3}]	1.458	1.531	1.496	1.490
μ [cm^{-1}]	11.73	12.39	11.88	13.52
Measured data	11013	10386	43489	18053
Data with $I > 2\sigma(I)$	5500	5132	8918	3858
Unique data/R_{int}	7136/0.0293	6813/0.0327	14280/0.0627	5955/0.0752
wR_2 (all data, on F^2)[a]	0.1312	0.0829	0.0832	0.1324
R_1 [$I > 2\sigma(I)$][a]	0.0465	0.0384	0.0382	0.0500
s[b]	1.022	1.025	0.962	1.019
Max/min residual density [e Å^{-3}]	1.844/–0.576	0.403/–0.459	0.673/–0.362	1.170/–0.506

[a] Definition of the R indices: $R1 = (\Sigma||F_o| - |F_c||)/\Sigma|F_o|$. $wR_2 = \{\Sigma[w(F_o2 - F_c^2)^2]/\Sigma[w(F_o^2)^2]\}^{1/2}$ with $w^{-1} = \sigma^2(F_o^2) + (aP)^2$. [b] $s = \{\Sigma[w(F_o^2 - F_c^2)^2]/(N_o - N_p)\}^{1/2}$.

least-squares techniques against F_o^2 (SHELXL-97[35]). All hydrogen atom positions were included at calculated positions with fixed thermal parameters. All non-hydrogen atoms were refined anisotropically.[36] XP (SIEMENS Analytical X-ray Instruments, Inc.) was used for structure representations. CCDC-753495 (**2a**), -753496 (**2b**), -753497 (**2c**), and -753498 (**3b**) contain the supplementary crystallographic data for this paper. These data can be obtained free of charge from The Cambridge Crystallographic Data Centre via www.ccdc.cam.ac.uk/data_request/cif.

Electrochemical Procedures: Cyclic voltammograms were recorded against a nonaqueous Ag/Ag$^+$ (0.1 M nBu$_4$NPF$_6$ and 0.01 M $AgNO_3$ in CH_3CN) or Ag/AgCl reference electrode. The Ag/Ag$^+$ reference electrode was used with acetonitrile, and the Ag/AgCl reference electrode was used when the electrochemical solvent was dichloromethane. Both reference electrodes were measured against the Fc/Fc$^+$ redox couple, and the potential values in Table 4 were all corrected against the Ag/Ag$^+$ reference. A glassy carbon (GC) macroelectrode and a platinum wire were used as the working and auxiliary electrodes, respectively. A solution of 0.05 M nBu$_4$NPF$_6$ (Fluka, electrochemical grade) in either acetonitrile (Aldrich, anhydrous, 99.8%) or dichloromethane (depending on the solubility of the compound) was used as the supporting electrolyte. Electrochemical experiments were carried out with a CHI750C electrochemical bipotentiostat. Prior to each experiment, the electrochemical cell was degassed by using argon for at least 10 min, and a blanket of argon was maintained throughout. The GC working electrode was prepared by successive polishing with 1.0 and 0.3 μm alumina pastes and sonicated in Millipore water for 5 min. All cyclic voltammograms were recorded at a scan rate of 100 mV s^{-1}.

Acknowledgments

Financial support for this work was provided by the Studienstiftung des Deutschen Volkes (U.-P. A.). Y. H. and J. G. V. thank the Science Foundation Ireland for financial support (grant no. 06/CHPRFP/029).

[1] Y. Nicolet, C. Piras, P. Legrand, C. E. Hatchikian, J. C. Fontecilla-Camps, *Structure* **1999**, *7*, 13–23.
[2] W. Peters, W. N. Lanzilotta, B. J. Lemon, L. C. Seefeldt, *Science* **1998**, *282*, 1853–1858.
[3] F. Gloaguen, J. D. Lawrence, M. Schmidt, S. R. Wilson, T. B. Rauchfuss, *J. Am. Chem. Soc.* **2001**, *123*, 12518–12527.
[4] M. Razavet, S. C. Davies, D. L. Hughes, J. E. Barclay, D. J. Evans, S. A. Fairhurst, X. Liu, C. J. Pickett, *Dalton Trans.* **2003**, 586–595.
[5] J. D. Lawrence, H. Li, T. B. Rauchfuss, M. Bernard, M. M. Rohmer, *Angew. Chem. Int. Ed.* **2001**, *40*, 1768–1771; H. Li, T. B. Rauchfuss, *J. Am. Chem. Soc.* **2002**, *124*, 726–727.
[6] L.-C. Song, Z. Y. Yang, H.-Z. Bian, Y. Liu, H.-T. Wang, X.-F. Liu, Q.-M. Hu, *Organometallics* **2005**, *24*, 6126–6135.
[7] J. Windhager, M. Rudolph, S. Bräutigam, H. Görls, W. Weigand, *Eur. J. Inorg. Chem.* **2007**, 2748–2760; L.-C. Song, Z.-Y. Yang, Y.-J. Huan, H.-T. Wang, Y. Liu, Q.-M. Hu, *Organometallics* **2007**, *26*, 2106–2110.
[8] U.-P. Apfel, D. Troegel, Y. Halpin, M. Rudolph, U. Uhlemann, M. Schmitt, J. Popp, H. Görls, P. Dunne, M. Venkatesan, M. Coey, J. G. Vos, R. Tacke, W. Weigand, *Inorg. Chem.* **2010**, DOI: 10.1021/ic101399k.
[9] R. S. Glass, N. E. Gruhn, E. Lorance, M. S. Singh, N. Y. T. Stessman, U. I. Zakai, *Inorg. Chem.* **2005**, *44*, 5728–5737.
[10] X. Zhao, I. P. Georgakaki, M. L. Miller, J. C. Yarbrough, M. Y. Darensbourg, *J. Am. Chem. Soc.* **2001**, *123*, 9710–9711.
[11] M. S. Arabi, R. Mathieu, R. Poilblanc, *J. Organomet. Chem.* **1979**, *177*, 199–209; K. Fauvel, R. Mathieu, R. Poilblanc, *Inorg. Chem.* **1976**, *15*, 976–978; J.-M. Savariault, J.-J. Bonnet, R. Mathieu, J. Galy, *C. R. Acad. Sci. Paris* **1977**, *284*, C663–C665.
[12] S. Ezzaher, J. F. Capon, F. Gloaguen, F. Y. Petillon, P. Schollhammer, J. Talarmin, *Inorg. Chem.* **2007**, *46*, 3426–3428; B. E. Barton, T. B. Rauchfuss, *Inorg. Chem.* **2008**, *47*, 2261–2263.
[13] W. Beck, W. Weigand, U. Nagel, M. Schaal, *Angew. Chem. Int. Ed. Engl.* **1984**, *23*, 377–378; W. Weigand, U. Nagel, W. Beck, *Z. Naturforsch. Sect. B: J. Chem. Sci.* **1988**, *43*, 328–338; W. Weigand, W. Beck, *Z. Anorg. Allg. Chem.* **1991**, *600*, 227–230; E. Bär, W. P. Fehlhammer, W. Weigand, W. Beck, *J. Org. Chem.*

1988, *347*, 101–106; C. Bianchini, F. Laschi, M. F. Ottaviani, M. Peruzzini, P. Zanello, F. Zanobini, *Organometallics* **1989**, *8*, 893–899; C. Nataro, J. B. Chen, R. J. Angelici, *Inorg. Chem.* **1998**, *37*, 1868–1875.
[14] F. Gloaguen, J. D. Lawrence, T. B. Rauchfuss, M. Bénard, M.-M. Rohmer, *Inorg. Chem.* **2002**, *41*, 6573–6582; F. Gloaguen, J. D. Lawrence, T. B. Rauchfuss, *J. Am. Chem. Soc.* **2001**, *123*, 9476–9477.
[15] P. Li, M. Wang, C. He, G. Li, X. Liu, C. Chen, B. Åkermark, L. C. Sun, *Eur. J. Inorg. Chem.* **2005**, 2506–2513.
[16] M. Nakamura, *Angew. Chem. Int. Ed.* **2009**, *48*, 2638–2640.
[17] P. I. Volkers, T. B. Rauchfuss, *J. Inorg. Biochem.* **2007**, *101*, 1748–1751.
[18] M. L. Singleton, N. Bhuvanesh, J. H. Reibenspies, M. Y. Darensbourg, *Angew. Chem. Int. Ed.* **2008**, *47*, 9492–9495.
[19] L.-C. Song, H.-T. Wang, J.-H. Ge, S.-Z. Mei, J. Gao, L.-X. Wang, B. Gai, L.-Q. Zhao, J. Yan, Y.-Z. Wang, *Organometallics* **2008**, *27*, 1409–1416.
[20] L. Schwartz, J. Ekström, R. Lomoth, S. Ott, *Chem. Commun.* **2006**, *40*, 4206–4208; S. P. Best, S. J. Borg, J. M. White, M. Razavet, C. J. Pickett, *Chem. Commun.* **2007**, *42*, 4348–4350; J. Windhager, U.-P. Apfel, T. Yoshino, N. Nakata, H. Görls, M. Rudolph, A. Ishii, W. Weigand, *Chem. Asian J.* **2010**, *5*, 1600–1610; P. C. Ellgen, J. N. Gerlach, *Inorg. Chem.* **1973**, *12*, 2526–2532.
[21] L.-C. Song, X.-F. Liu, J.-B. Ming, J.-H. Ge, Z.-J. Xie, Q.-M. Hu, *Organometallics* **2010**, *29*, 610–617.
[22] E. J. Lyon, I. P. Georgakaki, J. H. Reibenspies, M. Y. Darensbourg, *Angew. Chem. Int. Ed.* **1999**, *38*, 3178–3180; M. Schmidt, S. M. Contakes, T. B. Rauchfuss, *J. Am. Chem. Soc.* **1999**, *121*, 9736–9737; C. A. Boyke, J. I. van der Vlugt, T. B. Rauchfuss, S. R. Wilson, G. Zampella, L. De Gioia, *J. Am. Chem. Soc.* **2005**, *127*, 11010–11018.
[23] E. Lyon, I. P. Georgakaki, J. H. Reibenspies, M. Y. Darensbourg, *J. Am. Chem. Soc.* **2001**, *123*, 3268–3278.
[24] S. Ezzaher, P.-Y. Orain, J.-F. Capon, F. Gloaguen, F. Y. Petillon, T. Roisnel, P. Schollhammer, J. Talarmin, *Chem. Commun.* **2008**, 2547–2549.
[25] C. M. Thomas, T. B. Liu, M. B. Hall, M. Y. Darensbourg, *Inorg. Chem.* **2008**, *47*, 7009–7024; A. J. Justice, M. J. Nilges, T. B. Rauchfuss, S. R. Wilson, L. De Gioia, G. Zampella, *J. Am. Chem. Soc.* **2008**, *130*, 5293–5301; A. K. Justice, T. B. Rauchfuss, S. R. Wilson, *Angew. Chem. Int. Ed.* **2007**, *46*, 6152–6154; C. Tard, X. Liu, D. L. Hughes, C. J. Pickett, *Chem. Commun.* **2005**, 133–135; M. H. Cheah, C. Tard, S. J. Borg, X. Liu, S. K. Ibrahim, C. J. Pickett, S. P. Best, *J. Am. Chem. Soc.* **2007**, *129*, 11085–11092.
[26] K. Nakamoto, *Infrared and Raman Spectra of Inorganic and Coordination Compounds*, John Wiley, New York, **1986**.
[27] J. A. de Beer, R. J. Haines, R. Greatrex, N. N. Greenwood, *J. Chem. Soc. A* **1971**, *21*, 3271–3282; J. A. de Beer, R. J. Haines, *J. Organomet. Chem.* **1972**, *37*, 173–181.
[28] F. Gloaguen, D. Morvan, J. F. Capon, P. Schollhammer, J. Talarmin, *J. Electroanal. Chem.* **2007**, *603*, 15–20.
[29] D. Chong, I. P. Georgakaki, R. Mejia-Rodriguez, J. Sanabria-Chinchilla, M. P. Soriaga, M. Y. Darensbourg, *Dalton Trans.* **2003**, 4158–4163.
[30] T. Liu, M. Wang, Z. Shi, H. Cui, W. Dong, J. Chen, B. Akermark, L. Sun, *Chem. Eur. J.* **2004**, *10*, 4474–4479.
[31] A. Le Cloirec, S. C. Davies, D. J. Evans, D. L. Hughes, C. J. Pickett, S. P. Best, S. Borg, *J. Chem. Commun.* **1999**, 2285–2286.
[32] R. Mathieu, R. Poilblanc, P. Lemoine, M. Gross, *J. Organomet. Chem.* **1979**, *165*, 243–252.
[33] *COLLECT*, Data Collection Software, Nonius B. V., The Netherlands, **1998**.
[34] Z. Otwinowski, W. Minor in *Processing of X-ray Diffraction Data Collected in Oscillation Mode*, in *Methods in Enzymology*, vol. 276 (Macromolecular Crystallography, Part A) (Eds.: C. W. Carter, R. M. Sweet), Academic Press, New York, **1997**, pp. 307–326.
[35] G. M. Sheldrick, *Acta Crystallogr., Sect. A* **1990**, *46*, 467.
[36] G. M. Sheldrick, *SHELXL-97* (Release 97-2), University of Göttingen, Germany, **1997**.

Received: August 27, 2010
Published Online: December 12, 2010

